Vulnerability of OFDR-based distributed sensors to high γ-ray doses

S. Rizzolo,[1,2,3,*] A. Boukenter,[1] E. Marin,[1] M. Cannas,[2] J. Perisse,[4] S. Bauer,[3] J-R. Mace,[5] Y. Ouerdane[1] and S. Girard[1]

[1]*Laboratoire Hubert Curien, Université Jean Monnet, CNRS UMR 5516, 18 Rue Benoît Lauras, 42000, Saint-Etienne, France*
[2]*Dipartimento di Fisica e Chimica, Università di Palermo, Viale delle Scienze Parco d'Orléans II, Ed. 17, 90128 Palermo, Italy*
[3]*Areva Centre Technique, Boulevard de l'Industrie, 71200, Le Creusot, France*
[4]*Areva NP, 10 Rue Juliette Récamier, 69006, Lyon, France*
[5]*Areva NP, 1, Place Jean-Millier 92084, Paris-La Défense, France*
[*]*serena.rizzolo@univ-st-etienne.fr*

Abstract: Vulnerability of Optical Frequency Domain Reflectometry (OFDR) based sensors to high γ-ray doses (up to 10 MGy) is evaluated with a specific issue of a radiation-hardened temperature and strain monitoring system for nuclear industry. For this, we characterize the main radiation effects that are expected to degrade the sensor performances in such applicative domain: the radiation-induced attenuation (RIA), the possible evolution with the dose of the Rayleigh scattering phenomenon as well as its dependence on temperature and strain. This preliminary investigation is done after the irradiation and for five different optical fiber types covering the range from radiation-hardened fibers to highly radiation sensitive ones. Our results show that at these high dose levels the scattering mechanism at the basis of the used technique for the monitoring is unaffected (changes below 5%), authorizing acceptable precision on the temperature or strain measurements. RIA has to be considered as it limits the sensing range. From our vulnerability study, the OFDR sensors appear as promising candidates for nuclear industry even at doses as high as 10 MGy.

OCIS codes: (350.5610) Radiation; (290.5870) Scattering, Rayleigh; (060.2370) Fiber optics sensors.

References and links

1. S. Girard, J. Kuhnhenn, A. Gusarov, B. Brichard, M. Van Uffelen, Y. Ouerdane, A. Boukenter, and C. Marcandella, "Radiation effects on silica-based optical fibers: recent advances and future challenges," IEEE Trans. Nucl. Sci. **60**(3), 2015–2036 (2013).
2. http://www.iaea.org/
3. A. Morana, S. Girard, E. Marin, C. Marcandella, P. Paillet, J. Périsse, J.-R. Macé, A. Boukenter, M. Cannas, and Y. Ouerdane, "Radiation tolerant fiber Bragg gratings for high temperature monitoring at MGy dose levels," Opt. Lett. **39**(18), 5313–5316 (2014).
4. A. Faustov, "Advanced fibre optics temperature and radiation sensing in harsh environments" PhD Thesis (2014).
5. X. Phéron, S. Girard, A. Boukenter, B. Brichard, S. Delepine-Lesoille, J. Bertrand, and Y. Ouerdane, "High γ-ray dose radiation effects on the performances of Brillouin scattering based optical fiber sensors," Opt. Express **20**(24), 26978–26985 (2012).
6. C. Cangialosi, Y. Ouerdane, S. Girard, A. Boukenter, S. Delepine-Lesoille, J. Bertrand, C. Marcandella, P. Paillet, and M. Cannas, "Development of a temperature distributed monitoring system based on Raman scattering in harsh environment," IEEE Trans. Nucl. Sci. **61**(6), 3315–3322 (2014).
7. C. Cangialosi, S. Girard, A. Boukenter, M. Cannas, S. Delepine-Lesoille, J. Bertrand, P. Paillet, and Y. Ouerdane, "Hydrogen and radiation induced effects on performances of Raman fiber-based temperature sensors," J. Lightwave Technol. **33**(11), 1558–2213 (2015).

#238554 Received 22 Apr 2015; revised 23 Jun 2015; accepted 28 Jun 2015; published 15 Jul 2015

8. S. Kreger, D. Gifford, M. Froggatt, A. Sang, R. Duncan, M. Wolfe, and B. Soller, "High-resolution extended distance distributed fiber-optic sensing using Rayleigh backscatter," Proc. SPIE 6530, Sensor Systems and Networks: Phenomena, Technology, and Applications for NDE and Health Monitoring **2007**, 65301R (2007).
9. A. Faustov, A. Gusarov, L. B. Liokumovichc, A. A. Fotiadi, M. Wuilpart, and P. Mégret, "Comparison of simulated and experimental results for distributed radiation-induced absorption measurement using OFDR reflectometry," Proc. SPIE **8794**, 87943O (2013).
10. M. Van Uffelen, "Modélisation de systèmes d'acquisition et de transmission à fibres optiques destinés à fonctionner en environnement nucléaire" Ph.D. dissertation, Univ. de Paris XI, Paris, France, (2001).
11. D. L. Griscom, E. J. Friebele, K. J. Long, and J. W. Fleming, "Fundamental defect centers in glass: electron spin resonance and optical absorption studies of irradiated phosphorus-doped silica glass and optical fibers," J. Appl. Phys. **54**(7), 3743 (1983).
12. S. Girard, J. Keurinck, Y. Ouerdane, J.-P. Meunie, and A. Boukenter, "Gamma-rays and Pulsed X-Ray radiation responses of germanosilicate single-mode optical fibers:influence of cladding codopants," J. Lightwave Technol. **22**(8), 1915–1922 (2004).
13. Y. Sikali Mamdem, X. Phéron, F. Taillade, Y. Jaoüen, R. Gabet, V. Lanticq, G. Moreau, A. Boukenter, Y. Ouerdane, S. Delepine-Lesoille, and J. Bertrand, "Two-dimensional FEM analysis of Brillouin gain spectra in acoustic guiding and antiguiding single mode optical fibers" presented at COMSOL Conference, PARIS, 2010.
14. http://www.fibertronix.com/sites/default/files/datasheets/fibertronix-sm-high-temp-acrylate.pdf
15. F. Fernandez, H. Ooms, B. Brichard, M. Coeck, S. Coenen, F. Berghmans, and M. Décreton, "SCKCEN gamma irradiation facilities for radiation tolerance assessment" 2002 NSREC Data Workshop, **02HT8631**, 171–176 (2002).
16. H. Henschel, O. Kohn, and H. U. Schmidt, "Radiation induced loss measurements of optical fibres with optical time domain reflectometers (OTDR) at high and low dose rates" presented at the First European Conference on Radiation and its Effects on Devices and Systems, La Grande-Motte (1991).
17. R. H. West and S. Dowling, "Measurement of long term, radiation induced losses in fibre optics using optical time domain reflectometry" presented at the First European Conference on Radiation and its Effects on Devices and Systems, La Grande-Motte (1991).
18. S. T. Kreger, A. K. Sang, D. K. Gifford, and M. E. Froggatt, "Distributed strain and temperature sensing in plastic optical fiber using Rayleigh scatter," Proc. SPIE **7316**, 73160A (2009).
19. B. Soller, D. Gifford, M. Wolfe, and M. Froggatt, "High resolution optical frequency domain reflectometry for characterization of components and assemblies," Opt. Express **13**(2), 666–674 (2005).
20. B. J. Soller, M. Wolfe, and M. E. Froggatt, "Polarization resolved measurement of Rayleigh backscatter in fiber-optic components" presented at OFC Technical Digest, Los Angeles, 2005.
21. R. Duncan, B. Soller, D. Gifford, S. Kreger, R. Seeley, A. Sang, M. Wolfe, and M. Froggatt, "OFDR-based distributed sensing and fault detection for single- and multi-mode avionics fiber-optics," Joint Conference on Aging Aircraft. 2007.

1. Introduction

Silica-based optical fibers have recently attracted much interest for their use in harsh (in this paper, harsh is used for radiation) environments such as the ones encountered in space, military or high energy physics applications. Small size, fast response, light weight and immunity to electromagnetic fields are favorable advantages that often become decisive for fiber sensing to be chosen over other conventional sensing technologies. As an important and representative example, Fukushima's accident highlighted serious weaknesses in the safety of nuclear power plants. Since, one of the strategic research axis of the nuclear industry is devoted to the development of novel technologies and sensors to enhance and reinforce the safety in nuclear power plants, especially in the case of accidental conditions associated with a strong increase of the constraints applied to the fiber-based system [1,2].

The objective of this research field is to develop classes of distributed fiber-based sensors using scattering-based techniques, powerful solutions for distributed and local temperature, strain and radiation dose measurements. Optical fiber properties, indeed, depend on several external parameters such as temperature, strain and therefore the fiber itself can be used as the sensitive element. Different classes of fiber-based sensing techniques have been recently investigated such as Fiber Bragg Gratings (FBGs) for discrete measurements [3,4] and Brillouin [5], Raman [6,7] and Rayleigh [8,9] scattering based techniques for distributed measurements of various environmental parameters. Whereas Brillouin and Raman sensor resolutions remain in the range of one meter, the advantage of Rayleigh scattering based technique is that it offers very high spatial resolution from 1 cm down to few µm over several hundred meters of fiber length down to few meters respectively.

#238554 Received 22 Apr 2015; revised 23 Jun 2015; accepted 28 Jun 2015; published 15 Jul 2015

It is well known that irradiation induces point defects in the optical fiber core and cladding parts leading to an increase absorption and compaction phenomena. Among the classes of fibers Pure-silica core (PSC) and fluorine-doped (F-doped) optical fibers were known to present the highest radiation tolerance for high dose steady state exposure, exhibiting limited radiation-induced attenuation (RIA), especially in the infrared part of the spectrum where the OFDR systems operate [10]. These two classes of fibers are well known to be employed in the development of sensors in harsh environments even for distance up to kilometer. The presence of phosphorus, instead, induces the generation of specific point defects under irradiation having large absorption bands in both the visible and infrared parts of the spectrum that strongly reduce the fiber transmission [11]. These extremely radiation sensitive P-doped fibers are interesting candidates for the development of radiation detectors or dosimeters [1]. A. Faustov *et al.* demonstrate the potential of using P-doped fibers (or Al-doped ones) as sensitive parts of OFDR systems to monitor dose changes up to 20 Gy with a 15 cm resolution [9]. Germanosilicate optical fibers present intermediate radiation response in this dose range [10], they remain acceptable for some applications implying not too long fiber lengths, but it has been shown that the co-dopants present in their cladding could strongly change the RIA levels and kinetics, especially if phosphorus, even at low concentrations, has been incorporated [12].

For nuclear industry, integrating fibers-based sensors has to improve the performances (resolution, operating range,…) of security systems in current nuclear power plants (NPPs) and offers new alternative technologies that may overcome the issues identified for next generation of NPPs. Such integration will only be possible if the OFDR based systems are able to resist to the constraints associated with industrial environments, one of the most constraining being the presence of high level of radiations. It is known that radiations can modify the glass structure through its compaction or refractive-index changes. The amplitudes of these changes strongly depend on the nature of radiations. However, recent results have shown that at 10MGy γ-ray dose, the Brillouin properties of optical fibers could be affected [5], and as mentioned previously, this effect being also dependent on the fiber composition. In [5], a highly-germanium (photosensitive type) doped fiber was clearly more affected than the SMF28 Corning Telecom-grade fiber. For Rayleigh measurements the involved scattering mechanism differs from Brillouin ones and such a study is also mandatory before any sensor integration in nuclear facility. Rayleigh scattering is the elastic scattering that is generated by variation in a medium, such as the random refractive-index in homogeneities in glass or when the dimensions of particles are significantly smaller than the wavelength of the scattered light. In optical fibers, this effect induces a limitation to the fiber signal transmission, explaining that today's Telecom-grade optical fibers present losses of about 0.2dB/km in the third telecommunication window. However since the fluctuation of refractive index in a given fiber after its fabrication process remains fixed and as Rayleigh scattering in optical fiber is given by these fluctuations along the fiber length, techniques such as OFDR or OTDR (Optical Time Domain Reflectometry) are promising solutions for distributed measurements. Indeed, the physical length and refractive index of the fiber are intrinsically sensitive to the environmental parameters such as temperature and strain but also, even if to a lesser extent, to pressure, humidity, etc. All these parameters induce a change in scattered field. After calibration, this change is exploited for a distributed strain or temperature measurement. For a given and specific optical fiber, the corresponding OFDR based sensor should be calibrated in well controlled conditions of both temperature and strain in order to access to the evolutions of its optical responses under the considered solicitations and ranges. The open question being if at such MGy dose level radiations can affect distributed temperature and strain measurements.

In this paper, we are performing a systematic study to highlight the OFDR interest and sensitivity to probe the optical samples at high irradiation dose levels. This aspect is poorly discussed in literature even if a recent investigation was done in Belgium for low doses of

#238554 Received 22 Apr 2015; revised 23 Jun 2015; accepted 28 Jun 2015; published 15 Jul 2015

radiations (typically, below 100 kGy (SiO_2)) [4]. Degradation of such fiber sensors could be related to two different mechanisms. First, the radiation-induced attenuation that can limits the maximal length used in fiber sensor applications; another risk is that the radiation, by changing the glass matrix properties, changes the Rayleigh sensitivity to the two possible external solicitations: strain and temperature. As no results exist yet on the investigated dose range, we performed our study on pre-irradiated fibers (post-mortem measurements), focusing on permanent effects caused by the radiations. For RIA, these preliminary tests underestimate the online induced losses, whereas it seems that structural changes, if any, are more likely to be permanent. In that sense the results presented in this paper concerning the radiation effects on Rayleigh coefficient are assumed representative of those occurring during the irradiation.

2. Materials and methods

2.1 Investigated optical fibers

The responses of five optical fibers types were investigated in our study to explore the influence of both the material compositions and the γ-irradiation on the ODFR sensors (see Table 1). We first tested the commercial single mode fiber SMF28 from Corning which is commonly used in cable sensors considered as reference regarding our optical fibers set. Its radiation responses were already well discussed in terms of RIA [1] and Brillouin [5,13]. Two other germanosilicate prototype optical fibers from Alcatel were also investigated. The first (SMF3-Ge) one was a germanium (Ge)-doped fiber with a core size diameter of about ~10μm and a Ge concentration of ~6wt.% while the second (SMF4-GeP) is a germanium/phosphorus (GeP)-doped fiber similar to SMF3-Ge sample however the cladding is P-codoped (~0.3wt.%). Using these samples, we should highlight the influence of the Ge-concentration on the observed radiation-induced changes as well as the difference observed when the cladding is either radiation resistant or radiation sensitive. All Ge-doped fibers are surrounded with an acrylate coating adapted for temperatures up to 85°C.

To complete our samples set, two types of radiation resistant optical fibers have been characterized: (i) a single mode fiber (SMF) developed by iXFiber SAS manufacturer with a fluorine (F)-doped core of ~10μm diameter (SMF1-F); the fluorine concentration is about 0.2 wt.% in the core and ~1.8wt.% in the cladding. Its coating is also made of acrylate; (ii) a pure silica core (PSC) SMF fabricated by Fibertronix with a core diameter of ~8μm and a high temperature resistant acrylate coating, operating up to 150°C [14] (SMF2-PSC).

Table 1. List of investigated samples

Fiber	*Dopant in core*	*Dopant in cladding*	*Coating maximum operating temperature*
SMF28	Ge (~5wt.%)	Pure Silica	85°C
SMF1-F	F (~0.2wt.%)	F (~1.8wt.%)	85°C
SMF2-PSC	Pure Silica	Pure Silica	150°C
SMF3-Ge	Ge (~6wt.%)	Pure Silica	85°C
SMF4-GeP	Ge (~6wt.%)	P (~0.3wt.%)	85°C

2.2 Irradiation facilities

The γ-ray irradiations were performed using a ^{60}Co source facility (BRIGITTE) in SCK-CEN (Mol, Belgium) [15]. The dose-rate varies between 10 and 30 kGy/h, whereas the temperature ranges from 30°C to 50°C. The reached dose varies from 1 MGy up to a maximum of 10 MGy. All measurements were done typically one month after the end of the irradiation.

#238554 Received 22 Apr 2015; revised 23 Jun 2015; accepted 28 Jun 2015; published 15 Jul 2015

2.3 Radiation induced attenuation measurements

Radiation induced attenuation was measured to evaluated losses induced by radiation in investigated fibers along the whole samples length [16,17]. The optical fiber attenuation measurements were evaluated at 1550 nm with an Optical Time Domain Reflectometer (OTDR, EXFOFTB-7400E) in all studied samples (both pristine and irradiated ones) and the irradiation contribution (RIA) is deduced for each fiber type. All the measurements were carried out with a pulse width signal of 10 ns and an exposure time of 180 s; these parameters were chosen to probe fiber lengths even lower than 50 m.

2.4 Distributed sensing measurements

Distributed sensing measurements were done thanks to an Optical Backscatter Refectometer (OBR) 4600 from Luna Technologies. This OBR system uses swept-wavelength interferometry (SWI) to measure the Rayleigh backscattering as a function of length in optical fiber. The basic principle of this technique is to include the tested optical fiber in one arm of a Mach-Zender interferometer: the light of a tunable laser source is split and then recombined by two 3dB couplers. The detector is placed at the output of the second coupler and it detects fiber response in the frequency domain. Next a Fourier transform is performed to obtain the Rayleigh signature as a function of the fiber length [8]. A strain or temperature sensor is based on the response of Rayleigh scattering signature of the fiber under test (FUT) in both unperturbed (reference) and perturbed states. The scatter profiles from the two data sets are then cross correlated along the perturbed portion of the fiber to obtain the spectral shift in this part of the fiber due to a temperature or strain change. Rayleigh spectral shift exhibits a temperature and strain dependencies through Eq. (1):

$$\frac{\Delta\lambda}{\lambda} = -\frac{\Delta\nu}{\nu} = C_T \Delta T + C_\varepsilon \varepsilon. \tag{1}$$

Where λ and ν are the mean optical wavelength and frequency respectively; C_T and C_ε are temperature and strain calibration constants with typical values of $6.48 \cdot 10^{-6}$ $°C^{-1}$ and $0.780 \mu\varepsilon^{-1}$ for Germanium-doped silica core fibers [18–21]; ΔT and ε are the applied temperature and strain changes respectively. C_T and C_ε values are dependent on the dopant species and concentration in the fiber core, but also to a lesser extent on the cladding and coating compositions. The found spectral shift is then a measurement of the relative change in optical fiber obtained from applied perturbation and it does not give an absolute value of the absolute perturbation. OFDR distributed sensing measurements were performed to deduce the temperature and strain coefficients presented in Eq. (1) and therefore calibrate the sensor responses to these two solicitations. To this aim we developed two experimental set-ups that were optimized to measure the OBR response when the temperature (or the strain) applied to the fibers evolves. From the measurements done, the C_T and C_ε coefficients of a given fiber before and after irradiation are extracted and compared. In all measurements described below the laser source was tuned over a range of 21 nm with a center wavelength around 1550 nm (with an accuracy of 1.5 pm), yielding a nominal spatial resolution of the Rayleigh scatter pattern of 0.040 mm. The data acquisition rate limits maximum FUT range to roughly 70 m. Each measurement took less than 5 s for the 21 nm wavelength scan and associated calculations. Measurements were performed on a ~10 m long segment for temperature calibration and ~2m long segment for strain calibration measurements.

Temperature calibration was done in an oven controlled by a thermocouple; C_T was deduced from the slope of the Rayleigh spectral shift with temperature in the range from 30°C up to 80°C, where the last value is related to the maximal temperature the acrylate-based coatings can resist without impacting the fiber properties. For such experiments, all the samples of the same fiber type, both non-irradiated and irradiated ones, were spliced in series to perform the temperature treatment at the same time.

#238554 Received 22 Apr 2015; revised 23 Jun 2015; accepted 28 Jun 2015; published 15 Jul 2015

Strain was precisely induced by stretching the fiber with a translation set up coupled to an adapted tensile gauge for both the evaluation of the applied constraint and its stability during the measurement. The strain applied along the fiber is given in the relation: $\varepsilon = \Delta L/L$, were L is the length of stretched fiber (~50 cm). This measurement method was applied to all fiber samples, one after the other, under similar conditions. C_ε was deduced from the slope of the Rayleigh spectral shift with strain in the range from ~0 με up to 4500 με.

3. Experimental results

3.1 RIA

Attenuation measurements are reported in Fig. 1 from which we can estimate the dose dependency of permanent RIA at 1550 nm over 30 m long fibers (attenuation before irradiation, below 1dB/km is negligible). Different radiation sensitivities are shown depending on the nature of the dopants and their concentration in core and cladding.

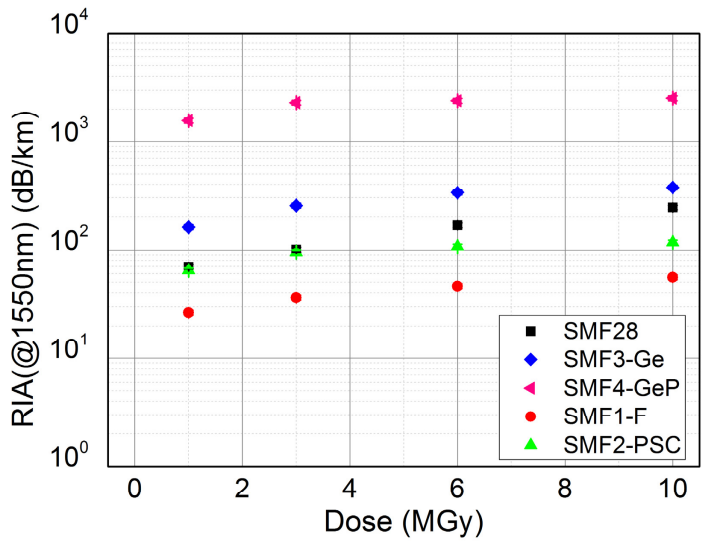

Fig. 1. Attenuation of studied optical fibers at 1550 nm irradiated at the doses of 1 MGy, 3 MGy, 6 MGy and 10 MGy.

F-doped and PSC fibers have lower losses with respect the others samples. At a total dose of 10 MGy, their corresponding amplitudes are 55 dB/km and 110 dB/km respectively. Whereas, highest RIA level is instead detected for GeP-doped fiber with ~2500 dB/km at 1550 nm. The RIA amplitudes in both SMF 28 and Ge-doped samples are ~250 dB/km and ~350 dB/ km respectively. These values agree with those reported in literature [1] and in particular we can point out the different effects of the dopants. Indeed, it is shown that the rule of fluorine makes fiber resistant to radiation; we found that the values of attenuation increase weakly increasing with the dose even for higher doses. The same behavior is shown from PSC fiber in which attenuation continues to grow weakly but the values are higher than F-doped. On the other hand the influence of phosphorus as co-dopant into the fiber cladding considerably reduces the fiber transmission down to zero after just few meters. The Ge concentration influence is also shown and evidenced from the comparison between SMF 28 and Ge fibers were increasing the Ge amount by1 wt.% enhances the radiation sensitivity of this class of fibers, as shown in [5] for another more highly-Ge doped sample.

#238554 Received 22 Apr 2015; revised 23 Jun 2015; accepted 28 Jun 2015; published 15 Jul 2015

3.2 Determination of temperature coefficients

In this part is presented the methodology whereby we calibrate the fiber to determine sensitivity coefficient that permits us to perform distributed measurements. In Fig. 2(a) is reported the spectral shift evaluated by the OBR system as a function of tested fiber length during the thermal treatments experiments used to determine the Rayleigh C_T. In this case (SMF 28 type), the fiber samples (of 2 meters length and irradiated up to 10 MGy dose) were spliced to each other in order to form one unique fiber (of 10 meters length) which will be submitted to the same thermal treatment in an oven (Binder) equipped with a type K thermocouple. The OBR measurements are performed with a spatial resolution of 1 cm at 10 different temperatures ranging from 35°C to 80°C, after a stabilization time of more than half an hour at each temperature step (of 5°C). Similar samples were prepared for other fiber types except for the GeP-doped one for which optical losses are too high to authorize simultaneous comparison between the non-irradiated fiber and its corresponding irradiated counterparts. In this case calibration was performed one sample after the other.

As the fiber was loosely placed into the oven, on the Fig. 2 we can distinguish direct temperature effect on the different parts of the fiber having been submitted to different irradiation doses. We can also recognize the locations of the splices along the path and also some stressed part (in particular for 6 MGy) that may due to some source of stress in this fiber zone that evolves with temperature and it is not eliminated by taking reference trace. Furthermore we note that the signal to noise ratio increases when the temperature of the oven increases. This last effect affects the whole fiber path and is assumed to be either related to slight vibrations of the fiber or to inhomogeneity of the temperature inside the oven (as reported in [4]). From Fig. 2(a), we can also directly notice that there are not obvious radiation effects on the spectral shift measured by our OBR system as for each part of the path, the signal evolves with temperature in the same way. From these data, we obtain the trend of spectral shift as a function of temperature shown in Fig. 2(b) for pristine and irradiated SMF 28 fiber. To calculate temperature coefficients we selected a range of length for each part of the sample (non-irradiated and irradiated) far from the splices and characterized by a low signal to noise ratio in order to eliminate some stress contributions that could misrepresent the final results; in each point of chosen range we calculated the coefficient thanks to a linear fit. Similar measurements were carried out on the other fibers to extract temperature coefficients for all the samples. We underline that for all the fibers (non-irradiated and irradiated) the spectral shift dependence on temperature is linear, as expected from literature [18–21].

All measurements of the spectral shift as a function of the temperature give us the information to obtain Fig. 3, where are shown the calculated temperature coefficients as a function of the dose for each fiber: SMF 28 Fig. 3(a), SMF1-F Fig. 3(b), SMF2-PSC Fig. 3(c), SMF3-Ge Fig. 3(d) and finally SMF4-GeP Fig. 3(e). In this figure the uncertainty on C_T values is calculated by an average analysis on the dispersion of temperature coefficient in different locations along the tested fiber. A list of all the coefficients with their relative errors is reported in Table 2.

#238554 Received 22 Apr 2015; revised 23 Jun 2015; accepted 28 Jun 2015; published 15 Jul 2015

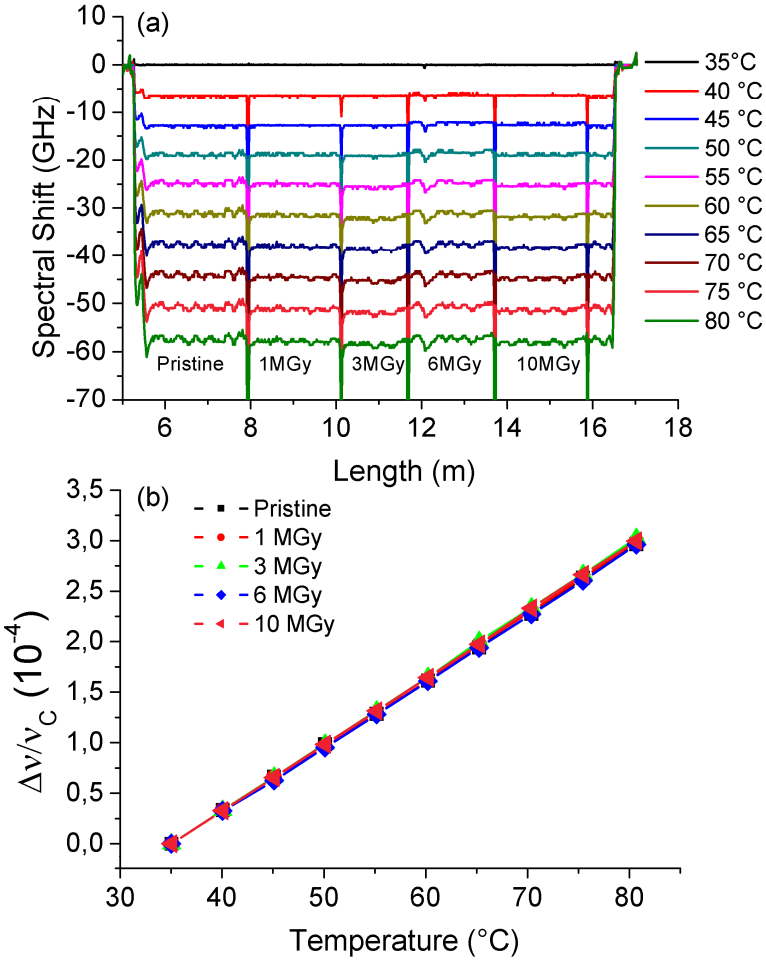

Fig. 2. Example of Rayleigh spectral shift in the fiber path of spliced SMF 28 (pristine and irradiated ones) as a function of the path length at 10 different temperatures from 35°C (reference trace) to 80°C and (b) measured Rayleigh spectral shift dependence on temperature for SMF28 pristine and irradiated samples at 1MGy, 3MGy, 6MGy and 10MGy shown for one point for each fiber in the considered range chosen to calculate C_T.

Table 2. Temperature coefficients extracted from Rayleigh measurements and relative errors

Dose (MGy)	*C_T (10^{-6}°C^{-1})*				
	SMF 28	*SMF1-F*	*SMF2-PSC*	*SMF3-Ge*	*SMF4-GeP*
0	6.47 ± 0.06	6.64 ± 0.02	6.44 ± 0.05	6.65 ± 0.03	6.46 ± 0.04
1	6.54 ± 0.03	6.30 ± 0.03	6.47 ± 0.03	6.81 ± 0.05	6.57 ± 0.02
3	6.63 ± 0.03	6.51 ± 0.04	6.49 ± 0.03	6.74 ± 0.03	6.68 ± 0.03
6	6.48 ± 0.04	6.80 ± 0.04	6.45 ± 0.03	6.57 ± 0.03	6.49 ± 0.02
10	6.59 ± 0.03	6.76 ± 0.04	6.36 ± 0.03	6.55 ± 0.03	6.49 ± 0.03

#238554 Received 22 Apr 2015; revised 23 Jun 2015; accepted 28 Jun 2015; published 15 Jul 2015

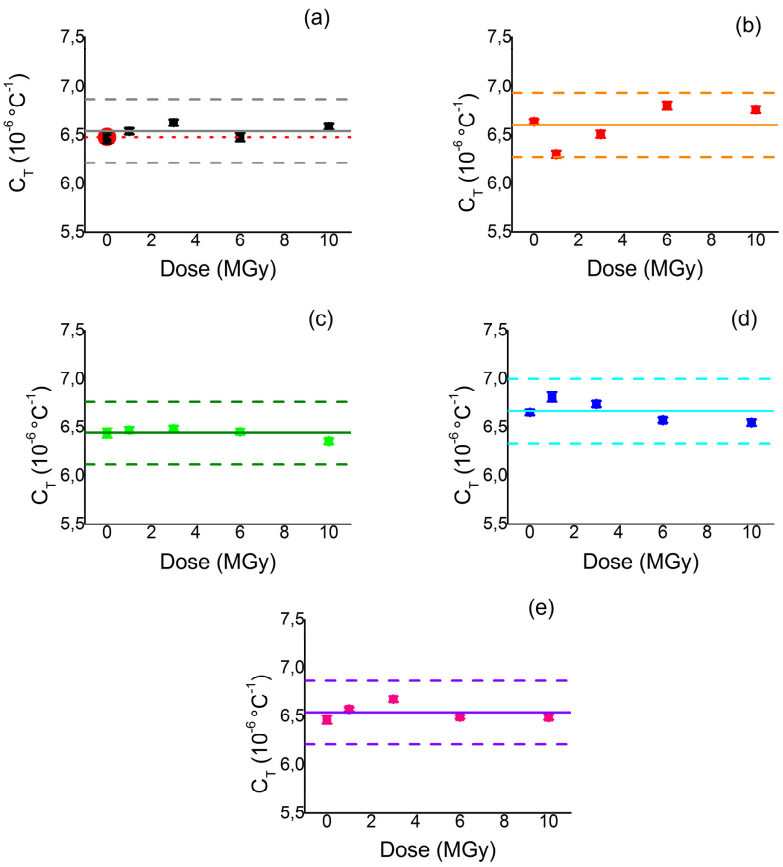

Fig. 3. Temperature coefficients extracted from Rayleigh spectral shift measurements as a function of irradiation doses in studied optical fibers: SMF 28 (a) in which is also represented the literature value [18–21] given as a red circle at 0MGy, SMF1-F (b), SMF2-PSC (c), SMF3-Ge (d) and finally SMF4-GeP (e). Solid line in the middle indicates the average values of the coefficients and space between dotted lines in each graph indicates a variation of 5% from average values that is the maximum variation obtained for the F-doped fiber.

No real radiation effect on C_T coefficient is highlighted from this large set of data. All the values are indeed scattered around the mean values (solid line in each graph) within a variation from 1% for the PSC fiber case up to a maximum of 5% for F-doped fiber. However, we note that this variation lead to an error on the temperature that grows with it; we calculate this error that varies from 0.1% for 35°C up to 0.6% for 80°C in the best case of PSC fiber and from 0.7% for 35°C up to 2.7% for 80°C in F-doped fiber that presents the wider range of C_T coefficients.

3.3 Determination of strain coefficients

Spectral shift as a function of fiber length (spatial sensing resolution of 2 mm) at different values of applied strain is reported in Fig. 4(a) for non-irradiated SMF 28 fiber; linear behaviors of spectral shift with applied strain in non-irradiated and irradiated samples of SMF 28 are instead shown in Fig. 4(b).

The strain coefficient was calculated taking the whole stressed part of the fiber shown in Fig. 4(a) as the trace is not noisy and only the strain effect is highlighted. As before for each point we verified that Eq. (1) is satisfied and we calculated the coefficient for each point

#238554 Received 22 Apr 2015; revised 23 Jun 2015; accepted 28 Jun 2015; published 15 Jul 2015

along the fiber thanks to a linear fit. These measurements were performed in stabilized temperature room with fluctuations in the order of ~0.1°C thanks to a J type thermocouple by TC Direct and repeated in the same conditions for all the fibers types at all the doses. Each curve show a linear trend as the one observed for SMF28 fiber.

An average analysis over the whole tested segment exposed to the strain (long of about 50 cm) leads us to compile Fig. 5 in which are reported the strain coefficients for all the fibers: non-irradiated and irradiated ones. In accordance with C_T determination, no real radiation effect on C_ε is observed even for the highest 10 MGy dose. The values are scattered around the mean values (solid line in each graph) within a variation from 1% that is the case of PSC fiber up to a maximum of 5% for SMF28 sample. This allows an error on strain measurements of 1% for PSC fiber up to 5% for SMF28. A list of all the coefficients with their relative errors is given in Table 3.

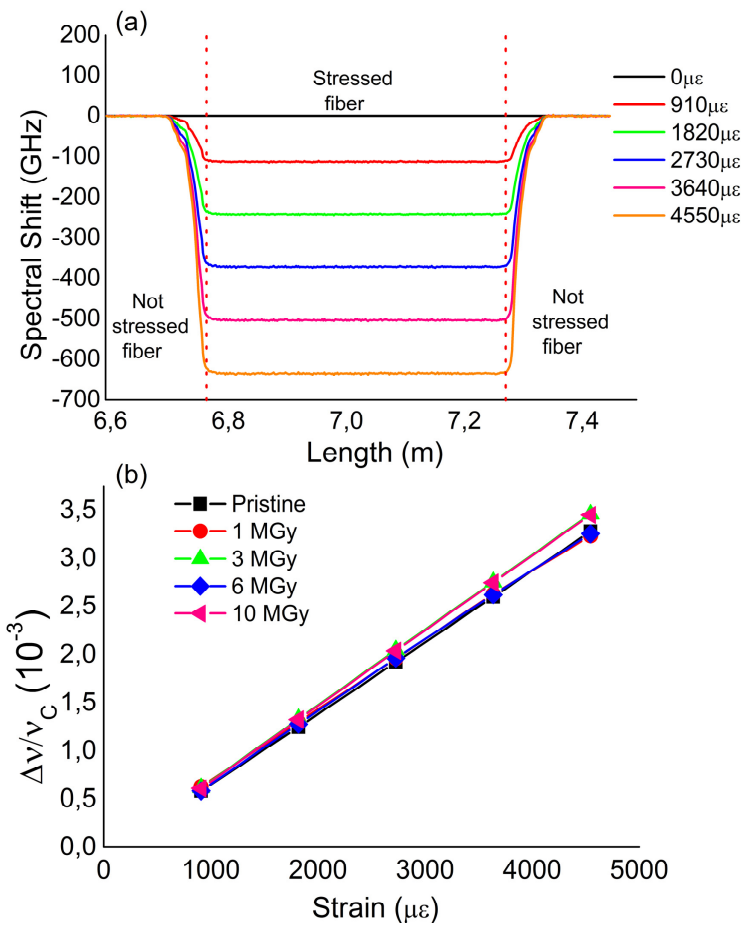

Fig. 4. (a) Example of Rayleigh spectral shift in SMF 28 sample as a function of fiber length at different applied strains from 0με (reference trace) up to 4550με and (b) measured Rayleigh spectral shift dependence on strain for SMF28 non-irradiated and irradiated samples at 1MGy, 3MGy, 6MGy and 10MGy shown for one point for each fiber in the considered range chosen to calculate C_ε.

#238554 Received 22 Apr 2015; revised 23 Jun 2015; accepted 28 Jun 2015; published 15 Jul 2015

Table 3. Strain coefficients extracted from Rayleigh spectral shift measurements and relative errors

Dose (MGy)	*C_ε ($\mu\varepsilon^{-1}$)*				
	SMF 28	*SMF1-F*	*SMF2-PSC*	*SMF3-Ge*	*SMF4-GeP*
0	0.743 ± 0.001	0.762 ± 0.002	0.801 ± 0.002	0.773 ± 0.002	0.759 ± 0.001
1	0.719 ± 0.001	0.736 ± 0.003	0.802 ± 0.001	0.742 ± 0.001	0.742 ± 0.001
3	0.783 ± 0.003	0.760 ± 0.001	0.799 ± 0.001	0.773 ± 0.002	0.779 ± 0.002
6	0.735 ± 0.002	0.784 ± 0.002	0.800 ± 0.002	0.740 ± 0.002	0.764 ± 0.001
10	0.781 ± 0.001	0.771 ± 0.002	0.799 ± 0.002	0.768 ± 0.002	0.747 ± 0.001

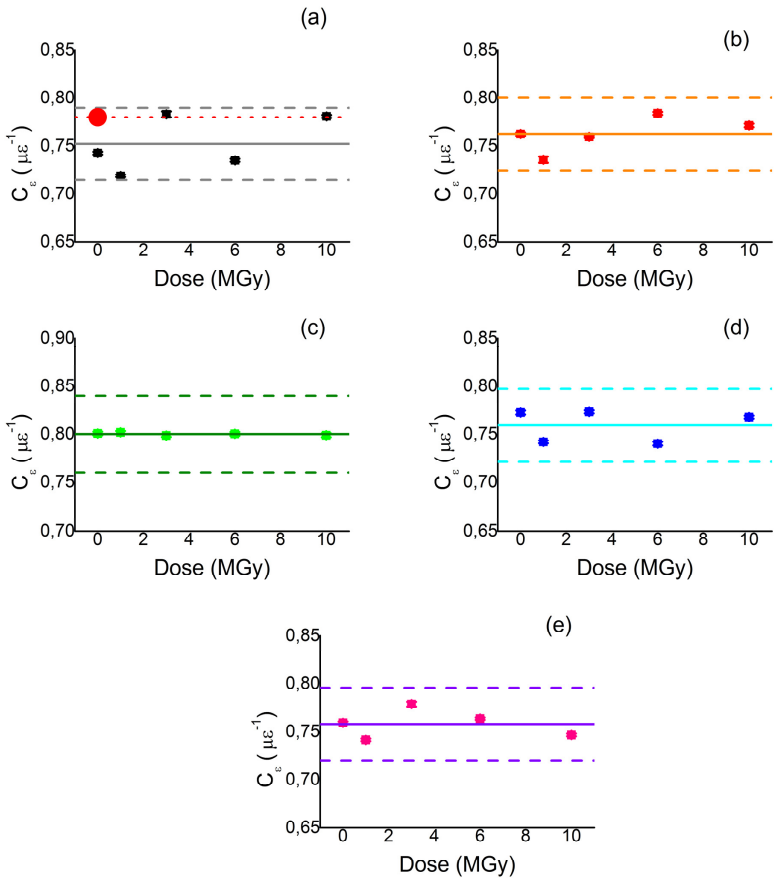

Fig. 5. Strain coefficients extracted from Rayleigh spectral shift measurements as a function of irradiation doses in studied optical fibers: SMF 28 (a) in which is also represented the literature value [18–21] given as a red circle at 0MGy and a dotted red line indicates in all the dose range, SMF1-F (b), SMF2-PSC (c), SMF3-Ge (d) and finally SMF4-GeP (e). Space between dotted lines in each graph indicates a variation of 5% from average values of the coefficients and solid line in the middle of this space indicates the average values of the coefficients.

4. Discussion

Our work is a detailed study on sensitivity of OFDR technique to high irradiation dose levels up to 10 MGy. This aspects, poorly discussed in literature, permits to investigate the

#238554 Received 22 Apr 2015; revised 23 Jun 2015; accepted 28 Jun 2015; published 15 Jul 2015

feasibility of distributed Rayleigh optical fiber based sensor in harsh environments. The two possible radiation induced mechanisms leading to the degradation of OFDR sensing performances are here discussed. First, in agreement with existing studies, radiation degrades the transmission properties of all fibers by creating point defects absorbing in the IR spectral range where OBR systems operate. Measured RIA in this domain (1550nm) through OTDR measurements give us induced losses with orders of magnitude going from ~50 dB/km in F-doped fiber up to ~2450 dB/km in GeP-doped ones. From OTDR results we confirm that both the nature and concentrations of dopants in the core and cladding of a fiber influence its radiation response. These measurements allow us to determine the maximal length that can be used in applications associated with such high doses of radiations and will permit to define our future online experiments. This information is useful because it points out the limits of OBR technique. Here we characterized five fibers that exhibit different responses to radiation: we tested a large set of fiber types including both radiation resistant ones and radiation sensitive samples. To highlight considerations pointed out from OTDR measurements we compare OBR trace in the two extreme classes of fiber: GeP and F; this information is reported in Fig. 6.

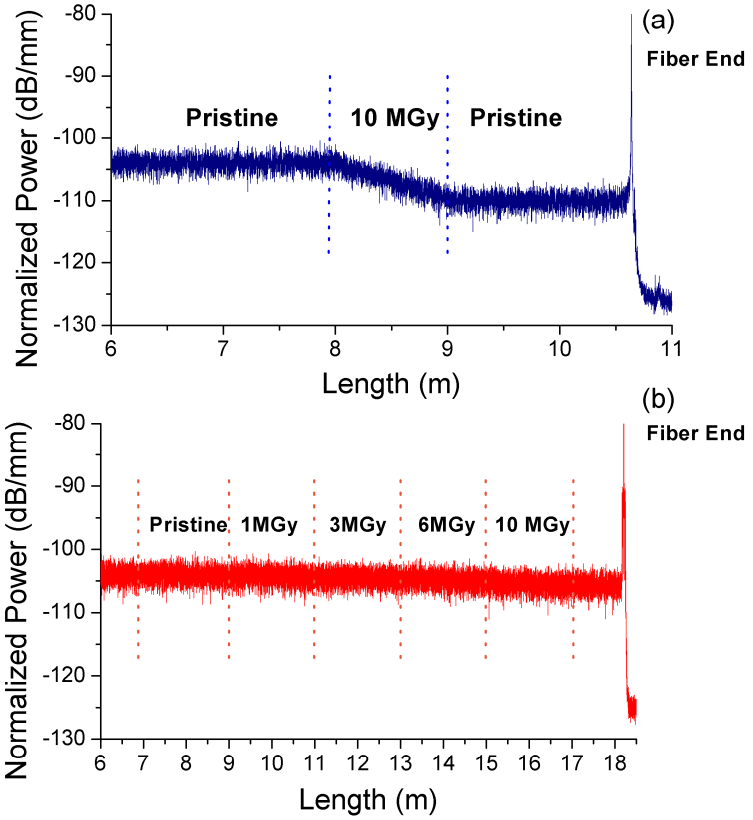

Fig. 6. Normalized power as a function of fiber length in GeP-doped fiber non-irradiated and irradiated at 10 MGy (a) and in F-doped fiber non-irradiated and irradiated at all the doses.

Normalized power of GeP-doped fiber non-irradiated and irradiated at 10 MGy Fig. 6(a) and of F-doped fiber non-irradiated and irradiated Fig. 6(b) as a function of fiber length show

#238554 Received 22 Apr 2015; revised 23 Jun 2015; accepted 28 Jun 2015; published 15 Jul 2015

that the GeP fiber response is so degraded due to RIA that even the trace of the OBR is affected whereas no modification can be distinguished in the F-doped fiber OBR trace. We can conclude that different fibers can be used for different purposes. In particular we found that for hardened temperature or strain distributed sensors, F-doped fibers appear to be very promising candidates; their low attenuation at 1550 nm up to 10 MGy permits their use for long sensing ranges under radiation without degradation of their C_T or C_ε coefficients. As reported in [9] for limited lower doses and for fibers with Al and P-doped cores, it seems possible to use the high radiation sensitivities of fibers to design a dosimeter. The authors of [4,9] however showed that for doses of the order of kGy, the sensing range is restricted to fiber length below 50 cm as for the investigated fibers, the signal amplitude gradually decreases down to OBR noise level. In our work we studied a GeP doped optical fiber that exhibits lower losses that a P-doped one, as only a minor part of the fundamental mode travels into the cladding; even if the employment of this fiber as a sensitive element is limited to few meters lengths, we conclude from this preliminary study that it may be possible to extend the dosimeter range up to 10MGy by optimizing the fiber composition and the whole sensor structure.

As final remarks, distributed measurements show that radiation does not affect temperature and strain measurements sensitivity. Different results were pointed out from a study on Brillouin scattering response to radiation [5]; in this work the authors showed that parameters are strongly affected by radiations that produce an error in the measure of the temperature of more than 20°C at the highest dose (10 MGy) for the most sensitive fibers. We found, instead, that C_T and C_ε have not a clear dependence with irradiation dose, and that the value is the same, within a 5% of error, for all the investigated types of fibers. Our study shows that this variation is not directly related to radiation since we measure the spectral shift eliminating all the permanent change due to radiation by performing a new reference trace.

5. Conclusion

In this paper, we performed a detailed study of the vulnerability of OFDR sensors to harsh environments associated with MGy dose levels. The potential of a large range of optical fibers for such applications has been investigated by using various fiber types, from radiation hardened to radiation sensitive ones. Our post mortem measurements show that the OFDR sensors are affected by the radiation induced attenuation (RIA) phenomena that limits their sensing range and degrade the signal-to-noise ratio. Some fibers, such as F-doped, may present RIA reduced to 55 dB/km which remains acceptable for the majority of applications targeted for these classes of sensors. Furthermore, our study demonstrates that the temperature and strain coefficients of the Rayleigh responses used for the monitoring of these two measurements remain unaffected by radiations up to 10 MGy. This opens the way to the development of radiation-tolerant OFDR systems for nuclear industries, high energy physics facility associated with high dose of radiations. As perspectives, the characterization of the OFDR sensors during the irradiation could be useful to ensure that no transient effect than RIA limits their performances and this for different temperatures of radiations.

#238554 Received 22 Apr 2015; revised 23 Jun 2015; accepted 28 Jun 2015; published 15 Jul 2015